Synthesis and characterization of a novel complex: Mo(CO)4-[2-(2′pyridyl)quinoxaline]. An insight based on experimental and theoretical data

Irene Veroni,[a] Aliki Rontoyianni[b] and Christiana A. Mitsopoulou *[a]

[a] Inorganic Chemistry Laboratory, Department of Chemistry, National and Kapodistrian University of Athens, Panepistimiopolis, Zografou 15771, Hellas.
E-mail: mitsopoulou@chem.uoa.gr
[b] Physical Chemistry Laboratory, Department of Chemistry, National and Kapodistrian University of Athens, Panepistimiopolis, Zografou 15771, Hellas

Synthesis and characterization of the new complex Mo(CO)4(2,2′-pq), where 2,2′-pq = 2-(2′pyridyl)quinoxaline, 1, is presented. The ligand 2,2′-pq, 2, belongs to the general class of quinoxalines, natural products yielding a rich coordination chemistry. This is the first reference for its coordination with Mo. Complex 1 crystallizes in space group $P2_1/n$ with $a = 9.621(4)$, $b = 16.748(7)$, $c = 10.343(4)$ Å, $Z = 4$ and $V = 1626.4(12)$ Å³. The octahedral geometry of the metal centre is distorted due to the bending of the axial carbonyls from the ligand 2. This bending is associated with the extensive solvatochromism of the MLCT band of complex 1 and related complexes as our semi-empirical calculations (ZINDO) and comparison with other complexes of Mo(CO)4L indicate. Moreover Oshika–Bayliss–McRae's formalism is employed in order to depict the solvation factors that influence the solvatochromism of 1. The latter one is attributed to the enhanced π-backbonding in 1, the polarization of the valence electrons of 2 and to the contribution of COs in the HOMO.

Introduction

Since the first report on the synthesis of Mo(CO)4phen by Hieber and Mühlbauer in 1935,[1] many papers on the study of zerovalent group 6 metal α,α′-diimine complexes of the type M(CO)4L have been published.[2] The continuing interest attracted to them is due not only to their role as starting materials for quite different classes of complexes, but also to their distinctive spectroscopic properties. Their photochemical and photophysical characteristics make their use quite essential in areas such as the investigation of polymerisation processes[3] and the exploitation of solar energy.[4] Their MLCT transitions could give rise to large microscopic second-order non-linearities (β_{ijk})[5] via a mechanism analogous to the charge-transfer excitations in organic non-linear optical (NLO) chromophores;[6] thus an application as NLO materials could be quite possible.

The structural simplicity of these complexes nominates them as ideal models for the understanding of the nature of MLCT transitions and their physical and chemical effects. The conclusions drawn from the study of the effect of the ligand L and the solvent on the tuning of their ground and excited state properties could reinforce the research on the molecular photonic and electronic devices.[7] Thus, there is a need, on the one hand, to investigate novel classes of organic ligands on the M(CO)4 fragments and, on the other, to approximate the mechanism of structural changes induced by solvent. Such approximations lead to subtle interpretations of their electronic absorption spectra.

Herein, we describe the synthesis and characterization of Mo(CO)4(2,2′-pq), 1, where 2,2′-pq is 2-(2′-pyridyl)quinoxaline, 2. This ligand was produced via an unusual condensation reaction from 2-acetylpyridine and 1,2-diaminobenzene[8a] and has been extensively studied because of its rich coordination chemistry in structural types and coordination modes.[8] 2-(2′-pyridyl)quinoxaline belongs to the general class of quinoxalines which are natural products,[9] used as antibiotics[10] and form polymers with peculiar magnetic and electric properties.[11] Their significant redox chemistry and photochemistry are responsible for many considerable intra- and inter-molecular electron transfer organic and biochemical processes.[12]

1

2
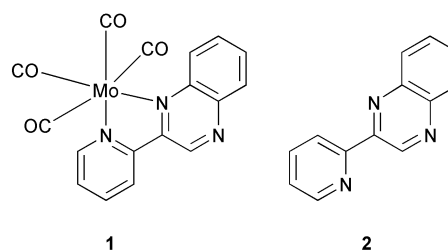
Furthermore, we analyze the crystal structure and associate it with the electronic spectrum of 1. The electronic spectrum is analyzed with the aid of semi-empirical calculations using the ZINDO method with CNDO/1 parameters.[13] A thorough examination of the effect of the type of solvent on the electronic absorption spectra of the complex, 'filtering' the data of the MLCT transition energies through McRae's solvent scale,[14] aims at gathering information on the ground state and the first MLCT excited state of 1. Finally, we reach several general conclusions about some of the factors that affect the size of the solvatochromism that is exhibited by the complexes of the type M(CO)4L.

Experimental

Materials

The metal hexacarbonyl complex Mo(CO)6 along with the reagent-grade solvents, which were used in the synthesis, were obtained from Aldrich Chemicals and used without further purification. The solvents used in UV-visible studies were purified to spectroscopic quality by standard methods.[15] The deuterated solvents, which were utilized in NMR experiments, were purchased by Aldrich and were of 99.99% purity. All reactions were carried out under typical Schlenk techniques.

Instrumentation

Electronic absorption spectra were recorded on a Varian Cary 300 spectrometer at 25 ± 0.2 °C. The solute concentration was

ca. 10^{-5} M and the samples were prepared a few seconds before the measurements. Infrared spectra were recorded as solid KBr discs on a Perkin Elmer Model 883 instrument using 2.40 cm^{-1} resolution. ^{1}H NMR measurements were performed using a Varian Unity Plus 300/54 NMR spectrometer. Samples were run in a 5 mm probe with deuterated solvents as internal lock and reference. The assignment of the ^{1}H NMR spectra of the free ligand L and of the complex was based on 2D NMR experiments (^{1}H–^{1}H COSY).

Synthesis

Syntheses of 2,2′-pq[8a] and Mo(CO)$_4$(piperidine)$_2$[16] were performed according to the literature methods.

Synthesis of 1. A mixture of 2,2′-pq (0.207 g, 1.00 mmol) and Mo(CO)$_4$(piperidine)$_2$ (0.378 g, 1.00 mmol) was stirred in methanol (20 ml) for 2 h at room temperature. The dark purple precipitate was filtered, washed with methanol and dried under vacuum.

Dark purple, prismatic crystals suitable for X-ray structural determination were obtained by re-crystallization during slow evaporation from a mixture of n-hexane–dichloromethane (4:1) at 279 K. Yield: 49%. Mp was not observed as **1** decomposes at 503 K. Found: C, 49.52; H, 2.15; N, 10.03. MoC$_{17}$H$_9$N$_3$O$_4$ requires: C, 49.18; H, 2.18; N, 10.12%.

IR $\tilde{\nu}_{CO}$/cm^{-1} (KBr disc): 2004$_s$, 1909$_{vs}$, 1866$_{vs}$ and 1822$_s$. δ_H(300 MHz, d$_6$-acetone): 10.01(s), 9.40(d), 9.19(d), 9.04(d), 8.35(tr), 8.27(d), 8.11(m), 7.82(tr).

Crystallography

Crystallographic data were collected on a Syntex P2$_1$ diffractometer with graphite monochromated Cu-Kα radiation at room temperature (293 K). Unit cell parameters were calculated from 36 reflections. 2310 Reflections were collected (θ_{max} = 58.5°), 2182 of which had $I > 2\sigma I$. Decay correction was applied.

The structure was solved by direct methods using the program SHELX-97.[17] At first, we defined the positions of molybdenum, of all atoms of the substituted quinoxaline, along with the positions of two oxygens. The positions of the other two oxygens and of the hydrogens were found from subsequent difference Fourier maps. The structure was refined in full-matrix least squares. Anisotropic thermal parameters were applied to all but hydrogen atoms. The final R factor was R = 0.0491 ($I > 2\sigma I$).

The structure and numbering scheme of the atoms of the complex are presented in Fig. 1. Table 1 contains the crystal data of the complex.
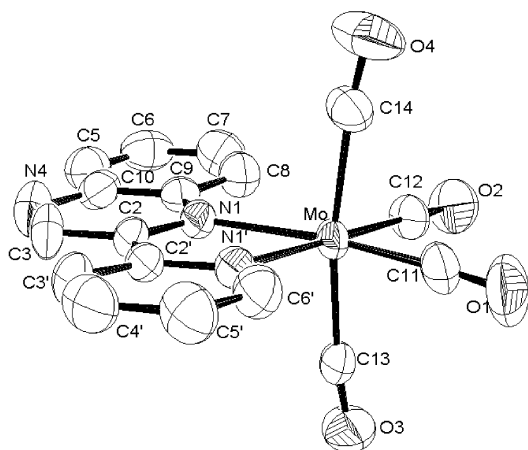

Fig. 1 ORTEP diagram of **1**.

Table 1 Crystallographic data for compound **1**

Formula	C$_{17}$H$_9$MoN$_3$O$_4$
M	415.21
Crystal system	Monoclinic
Space group	$P2_1/n$
a/Å	9.621(4)
b/Å	16.748(7)
c/Å	10.343(4)
β/°	102.604(15)
V/Å^3	1626.4(12)
T/K	293
Z	4
Total no. data	2310
Reflns. $I > 2\sigma I$	2182
R_{int}	0.0310
R	0.0491
wR	0.1385

CCDC reference number 193093.

See http://www.rsc.org/suppdata/dt/b2/b208769c/ for crystallographic data in CIF or other electronic format.

Computational details

The evaluation of the electronic spectrum of **1**, along with the assignment of its bands to certain transitions was accomplished *via* the application of the software package Quantum CACHe 3.2 of OxMol, which was run on a personal computer Pentium III 1000 MHz. Semi-empirical calculations were performed with the program ZINDO,[13] using CNDO/1 parameters, on the crystallographic structure of the complex.

Multiple regression analyses were carried out using the commercial StatGraphics Plus 4.0 software package.

Results and discussion

NMR spectroscopy

The complexation of 2-(2′pyridyl)quinoxaline to the Mo(CO)$_4$ moiety entails two major changes: the first involves the configuration of 2,2′-pq switching from the *syn/cis-* to the *anti/trans*-conformation, while the second is related to the withdrawal of electron density from it by the metal and at the same time a donation of partial charge back through the π-back-bonding. These changes are reflected on the NMR spectra of the complex. Fig. 2 displays the ^{1}H–^{1}H COSY spectra of the free ligand L and of the complex, which are important for assigning of the 1D-NMR peaks.

The NMR spectrum of the complexed ligand differs from that of the free ligand (Fig. 2), mainly due to the separation of H$_5$ and H$_8$ signals and to an overall downfield shift, which results from the stripping of electron charge off the ligand's protons after complexation. The most downfield shifted peak remains the H$_3$(s) followed by H$_6$′ and H$_8$, while H$_4$′ remains more downfield compared with H$_5$′.

Crystallographic analysis

The geometry of the complex is distorted octahedral. The atoms of molybdenum, of substituted quinoxaline and of C$_{11}$, C$_{12}$, O$_1$ and O$_2$ (*cis* carbonyls) lie on a plane[18] from which the highest deviation is that of the N$_1$′ atom (0.1153 Å). In Table 2, the most important bond lengths and angles are displayed. The distances within the coordinated 2-(2′-pyridyl)quinoxaline in **1** are in good correlation with the corresponding ones in the free ligand[8d] and in a number of pyridyl–quinoxaline complexes with different metals.[8c,f] An agreement in the relatively long bonds Mo–N and in the relatively small angle N–Mo–N also exists between **1** and other complexes of the type Mo(CO)$_4$L.[19]

The bond Mo–N$_1$ is *ca.* 0.10 Å longer than Mo–N$_1$′, something that implies a stronger bonding of Mo to the pyridyl than to the quinoxaline moiety of the ligand. At the equatorial

Table 2 Selected molecular parameters (distances in Å, angles in °) of compound **1**

Mo–N$_1$	2.300(4)	N$_1$–Mo–N$_1'$	72.48(15)
Mo–N$_1'$	2.220(4)	C$_{14}$–Mo–C$_{13}$	170.2(2)
Mo–C$_{11}$	1.943(6)	Mo–C$_{14}$–O$_4$	173.0(6)
Mo–C$_{12}$	1.974(5)	Mo–C$_{13}$–O$_3$	173.3(5)
Mo–C$_{13}$	2.033(6)	C$_{12}$–Mo–C$_{11}$	86.5(3)
Mo–C$_{14}$	2.042(6)	Mo–C$_{12}$–O$_2$	176.8(6)
C$_{11}$–O$_1$	1.167(8)	Mo–C$_{11}$–O$_1$	176.8(5)
C$_{12}$–O$_2$	1.138(7)	N$_1$–Mo–C$_{12}$	106.7(2)
C$_{13}$–O$_3$	1.135(7)	N$_1$–Mo–C$_{11}$	94.3(2)
C$_{14}$–O$_4$	1.137(8)	N$_1$–Mo–C$_{14}$	94.1(2)
C$_2$–C$_{2'}$	1.465(8)	N$_1'$–Mo–C$_{14}$	94.0(2)
N$_1$–C$_2$	1.322(7)	N$_1$–Mo–C$_{13}$	93.43(19)
N$_1'$–C$_{2'}$	1.360(7)	N$_1'$–Mo–C$_{13}$	94.25(19)

Fig. 3 Electronic absorption spectra of **1** in acetone (1), CHCl$_3$ (2) and n-heptane (3).
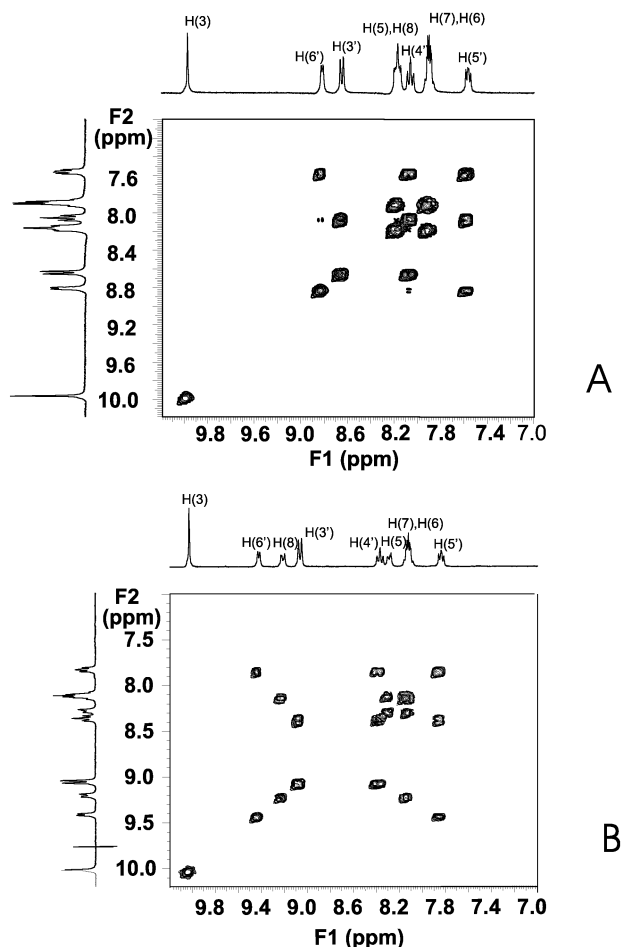

Fig. 2 COSY-NMR spectra of **2** (A) and **1** (B) in acetone.

plane, the bonds Mo–C$_{eq}$ are shorter (*ca.* 0.10 Å) and the bonds (C=O)$_{eq}$ longer (*ca.* 0.03 Å) than in the axial plane. This results from the smaller π-acidity of 2,2′-pq compared with that of a CO. The octahedral geometry of the metal centre is distorted mainly because of the small angle N$_1$–Mo–N$_1'$ and the bending of the axial carbonyls away from the ligand 2,2′-pq. The latter – which is also met in other complexes of this type [19] – affords an angle C$_{13}$–Mo–C$_{14}$ equal to 170° that probably is due to an electronic repulsion of the π* orbital of the diimine to the π* orbital of the axial COs.

UV-Vis spectroscopy

The electronic absorption spectra of Mo(CO)$_4$(2,2′-pq) in the area between 300 and 800 nm is characterized by two principal bands and a number of band-shoulders (Fig. 3). The higher energy band has a large ε (ε = 22 500 M^{-1} cm^{-1} in CHCl$_3$), and a spectral bandwidth of approximately 4200 cm^{-1}, while its maximum shows a slight solvent dependence and is positioned
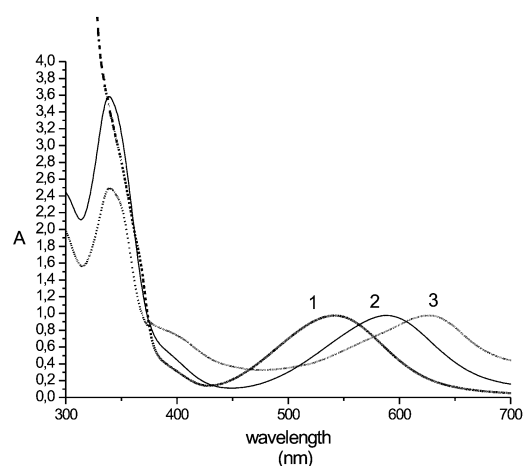
at 330–346 nm. The band's structure is solvent dependent as well as occasionally allowing the appearance of the shoulders at approximately 325, 375 and 400 nm. The lowest energy band has a smaller ε than the previous one – but this is still considerable, varying from 6880 M^{-1} cm^{-1} (CHCl$_3$) to 5200 M^{-1} cm^{-1} (acetone); its shape is quite symmetric in polar solvents, yet a higher energy shoulder appears in non-polar solvents that ruins the band's symmetry. As in other complexes of the type M(CO)$_4$L,[2] where L = α,α′-diimine, this band has a MLCT character and exhibits a significant negative solvatochromism; its maximum shifts to higher energies in solvents of increasing polarity.

In an attempt to gain some understanding of the solvatochromic behaviour of the complex, whose colour ranges from pink to a greenish colour (*ca.* 3346 cm^{-1} range) depending on the solvent: firstly we recorded its absorption spectra in 25 different solvents, and the frequencies of the solvatochromic band maxima (cm^{-1}) are registered in Table 3; and secondly the theoretical electronic spectrum of **1** was calculated with the aid of the ZINDO program. Despite the effective prediction of the general pattern of the experimental spectrum, the precision of the maximum of the MLCT band was not so accurate. Nevertheless, as the calculations indicate, the LUMO consists of mainly the π* orbital of 2,2′-pq while the HOMO contains, apart from the d$_\pi$ orbital of the metal, the contribution from the carbonyl π* orbitals. Several other M→diimine MLCT transitions were calculated to lie in the energy range of the visible absorption band which has CO character in both the HOMO and LUMO. However, owing to their very low intensities they contribute only the broadening of the band and to its low energy tail. Although ZINDO calculations are not precise these results are not in contradiction to those that were obtained by means of DFT formalism for analogous complexes of Cr and W.[20] As a matter of fact, the contribution of CO ligands – which probably appears in most of the complexes of the type M(CO)$_4$L – was first recognized with the aid of resonance Raman spectroscopy,[21] and was further verified by DFT calculations on representative complexes of this type.[7,22,23]

The extent of the contribution of the carbonyl ligands to the HOMO (or LUMO)[20] is expected to be related to the geometry of the complexes and in particular to the angle between the axial carbonyls and the central metal. Moreover it should influence the extent of solvatochromism that appears. Thus the angle C–M–C and extent of solvatochromism should be related. To make this point more tangible we have compared the C$_{axial}$–M–C$_{axial}$ angle to the extent of solvatochromism for some Mo complexes (Table 4). We focus on Mo complexes since a change of the metal could influence the size of the angle. It is clear that the smaller the angle, the bigger the observed solvatochromism. Considering that the bending of the axial

Table 3 Maximum absorbance frequencies of MLCT transitions of **1** in various solvents. The values of the dipole moment μ, dielectric constant ε, refractive index n_D^{20}, and of the characteristic functions met in McRae's equation of the corresponding solvents

Solvent	μ/D	ε	n_D^{20}	$(n^2 - 1)/(2n^2 + 1)$	$(\varepsilon - 1)/(\varepsilon + 2) - (n^2 - 1)/(n^2 + 2)$	$\tilde{v}$ MLCT/cm^{-1}
Methanol	2.97	32.630	1.326	0.167888	0.711608	17953
Ethanol	1.71	24.300	1.359	0.180427	0.665784	17575
Acetonitrile	3.39	37.500	1.342	0.173898	0.713547	18784
Acetone	3.11	20.700	1.356	0.179314	0.649349	18517
THF	1.69	7.580	1.404	0.196506	0.442284	17751
Chloroform	1.11	4.806	1.444	0.209880	0.293582	16979
Carbon tetrachloride	0.00	2.238	1.459	0.214686	0.018743	15976
DMSO	3.90	46.680	1.477	0.220401	0.655662	18986
Toluene	0.37	2.438	1.494	0.225479	0.032898	17007
DMF	3.82	36.710	1.428	0.204696	0.665120	18772
Diethyl ether	1.23	4.335	1.353	0.178084	0.309772	17027
Dichloromethane	1.90	9.100	1.421	0.202291	0.476139	17626
n-Heptane	0.00	1.920	1.385	0.189855	0.000347	15993
Iso-octane	0.00	1.940	1.392	0.192153	0.000721	15738
Acetic acid	—	6.150	1.370	0.184463	0.405716	17452
Cyclohexanone	3.07	18.300	1.448	0.211172	0.584513	18028
Benzene	0.00	2.284	1.498	0.226677	0.006600	17123
m-Xylene	—	2.374	1.495	0.225779	0.022507	16949
Piperidine	1.19	5.800	1.453	0.212617	0.345355	17422
Methyl ethyl ketone	2.78	18.510	1.379	0.187642	0.622746	18248
3-Pentanone	2.72	17.000	1.392	0.192469	0.603763	18058
Methyl isobutyl ketone	—	13.110	1.396	0.193799	0.561070	17929
Carbon disulfide	0.00	2.641	1.628	0.261934	−0.001300	15964
n-Hexane	0.08	1.890	1.372	0.185189	0.001513	15640
Nitromethane	3.46	35.870	1.380	0.188072	0.689146	18695

Table 4 Comparison between the angle C_{axial}–Mo–C_{axial} and the extent of solvatochromism $\Delta\tilde{v}$ (for two solvents: methanol and toluene) for some tetracarbonyl-α,α'-diimine complexes of Mo

Complex[a]	C_{axial}–Mo–C_{axial}/°	$\Delta\tilde{v}$/cm^{-1}
Mo(CO)$_4$(phen) [19a,24]	167.6	1570
Mo(CO)$_4$(pyca-β-ala-OEt) [19e]	167.7	1283
Mo(CO)$_4$(dab) [19f]	169.6	1304
Compound **1**	170.2	946

[a] phen = phenanthroline; pyca = pyridinecarbaldehyde imine; dab = diazabutadiene.

carbonyls backwards to the diimine is a consequence of the repulsion of the electrons of the diimine's π* orbital, we suggest that the size of the C–M–C angle gives an indication of the changes of dipole moment during the MLCT transition. More advanced calculations for all these complexes, for example DFT, could justify the accuracy of this hypothesis.

Solvatochromic data analysis

According to the theory of dielectric polarization,[25] negative solvatochromism is expected for transitions from a state with a high dipole moment to a state with a smaller one. This keeps up well with the general conception that the solvent dependence of the complexes of the type M(CO)$_4$L, where L = α,α'-diimine, is due to the fact that these complexes are highly polar and that the transition moment of the MLCT transition lies antiparallel to the ground state dipole moment.[26] This in turn results in a more polar ground state (GS) than an excited state (ES), and an enhanced stabilization of the GS by the (di)polar solvents leading to an increased transition energy.

In order to interpret the solvatochromic behaviour of Mo(CO)$_4$(2,2'-pq), we focused on the higher wavelength absorption transition which according to previous literature on complexes of the same type[2] and our theoretical studies on this particular complex, has MLCT character. The frequencies of the MLCT absorption maxima vary in accordance with the interactions of the dipole moment of the solute molecule with the reaction field[27] induced by the surrounding solvent and to the short-range specific effects such as the hydrogen bonds. The very good correlation of $\tilde{v}_{max}$ with the dipole moment μ of the
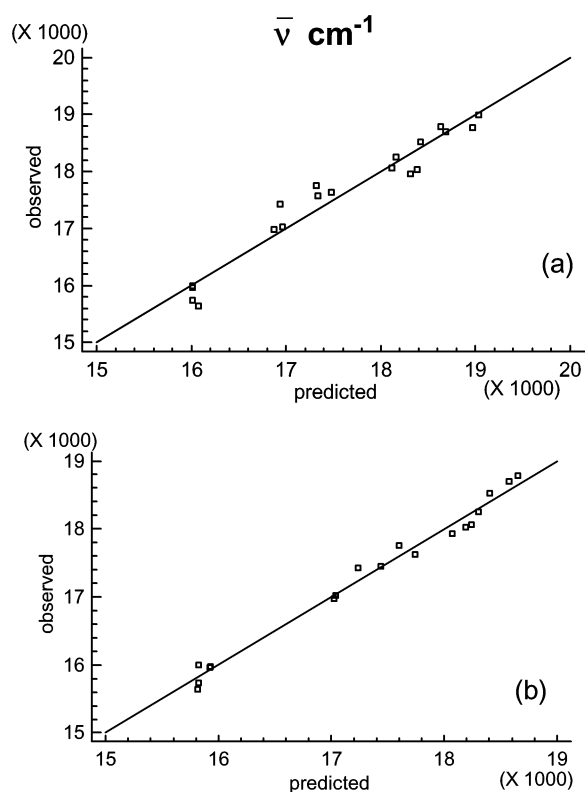

Fig. 4 Calculated *vs.* observed transition energies for MLCT of **1**: (a) according to the dipole moment of the solvents; (b) to McRae's formalism.

solvent used, after the omission of the aromatic solvent data (Table 5, Fig. 4), verifies the major contribution of dipolar interactions to the solvatochromic behaviour of the complex. The poor correlation when the aromatic solvents are taken into consideration in the data analysis stems from the anisotropic effect they exhibit on solute's properties; these may also indicate a π–π interaction of the aromatic cloud of 2,2'-pq with the solvent's one. The positive sign of the coefficients in the equations $\tilde{v}_{max} = f(\mu)$ (Table 5) indicates that the MLCT trans-

Table 5 Results of regression analyses on MLCT transition frequencies of **1**[a]

Independent variable	Entry	Solvent set	a^b	β^b	$(A + B)^c$	C^c	D^c	R^2
μ	1	All	705.34 ± 54.31 (0.0000)[d]	16214.0 ± 121.4 (0.0000)[d]				0.8940
	2	Non-ArH	773.984 ± 41.01 (0.0000)[d]	16011.0 ± 96.1 (0.0000)[d]				0.9519
McRae terms: $\dfrac{(n^2-1)}{(2n^2+1)}$ $\left[\dfrac{(\varepsilon-1)}{(\varepsilon+2)}-\dfrac{(n^2-1)}{(n^2+2)}\right]$	3	All			11285 ± 4325 (0.0160)[d]	3647 ± 325 (0.0000)[d]	13806 ± 939 (0.0000)[d]	0.8641
	4	Non-ROH, non-ArH			3941 ± 2077 (0.0750)[d]	4203 ± 155 (0.0000)[d]	15006 ± 438 (0.0000)[d]	0.9787
	5	Non-ROH, non-ArH, DMSO, DMF			1467 ± 1794 (0.4263)[d]	4000 ± 137 (0.0000)[d]	15541 ± 380 (0.0000)[d]	0.9855

[a] Data are taken from Table 3. [b] a and β stand for the coefficient and the constant, respectively, in the equation: $\tilde{v}_s = a\mu + \beta$. [c] $(A + B)$, C and D are the two coefficients and the constant, respectively, in McRae's equation: $\tilde{v}(S) = (A + B)[(n^2 - 1)/(2n^2 + 1)] + C[(\varepsilon - 1)/(\varepsilon + 1) - (n^2 - 1)/(n^2 + 2)] + D$. [d] The terms in parentheses correspond to the statistical p-value for each coefficient and constant.

ition energy increases as the solvents get more polar. This, of course, corresponds to the negative solvatochromism of the complex.

However satisfactory the above correlation results may be, the correlation to μ does not allow us to picture the solvation factors that influence the shift of the MLCT transition of the complex, as we only consider the dipole–dipole part of van der Waals solute–solvent interactions, neglecting the dipole-induced dipole interactions and London's dispersion forces. To overcome this and simultaneously improve the linear correlation results, we treat the solvatochromic shifts using Oshika–Bayliss–McRae's formalism.[14] Within that framework, which is an extension of Onsager's reaction field theory,[28] the frequency $\tilde{v}(S)$ of the solvatochromic band of a given indicator in solvent S is now provided by eqn. (1):

$$\tilde{v}(S) = (A + B)[(n^2 - 1)/(2n^2 + 1)] + C[(\varepsilon - 1)/(\varepsilon + 1) - (n^2 - 1)/(n^2 + 2)] + D \quad (1)$$

where the first term expresses the dispersion and induction forces and the second the dipole–dipole interactions. The coefficient C expresses the dipole moment change between the ground and the excited states of the solute and it is equal to

$$C = (2\pi\varepsilon_0 cha^3)^{-1}\mu_g(\mu_g - \mu_e) \quad (2)$$

where μ_g and μ_e are the dipole moment (in Cm) of ground and excited states, respectively; $\varepsilon_0 = 8.854 \times 10^{-12}$ J^{-1} C^2 m^{-1}; $h = 6.63 \times 10^{-34}$ Js; $c = 3.0 \times 10^8$ m s^{-1}; a is the radius of solute's cavity.

Applying a multiple regression analysis using $(n^2 - 1)/(2n^2 + 1)$ and $[(\varepsilon - 1)/(\varepsilon + 1) - (n^2 - 1)/(n^2 + 2)]$ as independent variables and $\tilde{v}_{max}$ as the dependent variable (their values are contained in Table 3), we obtained the results of Table 5. The values attained by the coefficient $(A + B)$ of the model are very sensitive to the choice of solvent group. After omitting the data for aromatic solvents, alcohols, DMSO and DMF, the coefficient $(A + B)$ becomes quite insensitive to any change in the solvent group. In the original paper of McRae the alcohol group of the solvent is excluded from the data set, along with any other solvent group that interacts with the solute in a specific way by short-distance forces. So the omission of the particular solvents mentioned above improves the fitting procedure and generates equations with interesting physical interpretations.

Examining entry 5 of Table 5 we conclude from the values of the coefficients in McRae's eqn. (1) that the contribution of the dipolar term is much more significant than the dispersion and induction terms. Therefore the complex's solvatochromism is defined by the dipole–dipole interactions with the solvent. The large p-value for the $(A + B)$ coefficient indicates that the dispersion and induction term may be omitted – retaining only the dipolar term. Despite this, we decided not to proceed with this omission, as it would suppress the physical significance of McRae's equation. Thus, eqn. (1) and more specifically entry 5 of Table 5 will be used for the description the solvatochromism of **1**.

Taking bibliographic information for $\tilde{v}_{max}$ of the complex $Mo(CO)_4(phen)$ in various solvents,[24] we apply McRae's equation and obtain a value for C of 6412 (±167) cm^{-1}, while for $Mo(CO)_4(bpm)$ a value of 5490 (±365) cm^{-1} is obtained.[26b] These data, along with the corresponding value for **1** (4000 ± 203), point out that $Mo(CO)_4(phen)$ appears to exhibit the greatest extent of solvatochromism (Table 4) among the analogous Mo compounds.

The factors that contribute to the smaller ground-excited dipole moment change of **1** relative to that of $Mo(CO)_4(phen)$ could have as origin the enhanced π-backbonding in **1**, improving the coupling between the donor and the acceptor, the easier the polarization of the valence electrons[29] of 2,2′-pq and the less important contribution of the carbonyls in the HOMO of complex **1** ascribed to the magnitude of the C–M–C angle. As far as the third factor is concerned, the participation of the carbonyls seems to move the centre of electron donation further away from the centre of electron acceptance that is situated on the α,α′-diimine. Therefore the effective distance between the electron donor and the acceptor, during the MLCT transition, increases and consequently the dipole moment change is enhanced. In other words, the so called MLCT excitation concerns the whole $Mo(CO)_4(diimine)$ molecule and not just the $Mo(diimine)$ fragment as is usually assumed. These observations are consisted with the ones that have been reported for $Cr(CO)_4(bpy)$.[23]

Conclusions

The synthesis, characterization and crystallographic analysis of a novel complex $Mo(CO)_4(2,2′\text{-pq})$ is presented. Exploiting the Oshika–Bayliss–McRae formalism the extensive solvatochromic effect of its MLCT band is investigated in order to depict the solvation factors and to estimate the dipole moment change between the ground- and the excited-states of the solute. Moreover, the crystal data and especially the bending of axial

COs, along with semi-empirical calculations (ZINDO), and comparison with data from other $Mo(CO)_4$(α-diimine) complexes are employed for the explanation of the difference on the dipole moment change during the MLCT transition. Contrary to a conventional view and in agreement with the results for the analogous Cr complex,[23] it is suggested that during the MLCT excitation electron density is minimized both to the metal and axial carbonyls.

Acknowledgements

References

1 W. Hieber and F. Mühlbauer, *Z. Anorg. Allg. Chem.*, 1935, **221**, 337.
2 D. J. Stufkens, *Coord. Chem. Rev.*, 1990, **104**, 39.
3 A. J. Lees, *Coord. Chem. Rev.*, 1998, **177**, 3.
4 V. Balzani, A. Juris, M. Venturi, S. Campagna and S. Serroni, *Chem. Rev.*, 1996, **96**, 759.
5 D. R. Kanis, M. A. Ratner and T. J. Marks, *J. Am. Chem. Soc.*, 1990, **112**, 8203.
6 J. Messier, F. Kajar, P. Prasad and D. Ulrich, *Nonlinear Optical Effects in Organic Polymers*, Kluwer Academic Publishers, Dordrecht, 1989; D. J. Williams, *Angew. Chem., Int. Ed. Engl.*, 1984, **23**, 690.
7 I. R. Farrell, F. Hartl, S. Záliš, T. Mahabiersing and A. Vlček, Jr., *J. Chem. Soc., Dalton Trans.*, 2000, 4323.
8 (*a*) S. Kasselouri, A. Garoufis, A. Katehanakis, G. Kalkanis, S. P. Perlepes and N. Hadjiliadis, *Inorg. Chim. Acta*, 1993, **207**, 255; (*b*) J. C. Plakatouras, N. Hadjiliadis, S. P. Perlepes, A. Albinati and G. Kalkanis, *Polyhedron*, 1993, **12**, 2069; (*c*) E. G. Bakalbassis, J. Mrozinski, S. P. Perlepes, N. Hadjiliadis, F. Lianza and A. Albinati, *Polyhedron*, 1994, **13**, 3209; (*d*) S. Kasselouri, A. Garoufis, S. Paschalidou, S. P. Perlepes, I. S. Butler and N. Hadjiliadis, *Inorg. Chim. Acta*, 1994, **227**, 129; (*e*) A. Garoufis, S. P. Perlepes, A. A. Froystein, J. Sletten and N. Hadjiliadis, *Polyhedron*, 1996, **15**, 1035; (*f*) A. Garoufis, A. Koutsodimou, C. P. Raptopoulou, A. Simopoulos and N. Katsaros, *Polyhedron*, 1999, **18**, 3005.
9 M. G. Knize, C. P. Salmon and E. C. Hopmans, *J. Chromatogr., A*, 1997, **763**, 179.
10 F. F. Seelig, *Z. Naturforsch., A*, 1979, **34**, 986; N. E. Mollegaard, C. Bailly, M. J. Waring and P. E. Nielsen, *Biochemistry*, 2000, **39**, 9502; H.-R. Park, T. H. Kim and K.-M. Bark, *Eur. J. Med. Chem.*, 2002, 1.
11 M. Inoue and M. Kubo, *Coord. Chem. Rev.*, 1976, **21**, 1; E. Hyde, J. R. Kalman, D. H. Williams, D. G. Reid and R. K. Olsen, *J. Chem. Soc., Perkin Trans. I*, 1982, 1041; Z. Kucybala, I. Pyszka and J. Paczkowski, *J. Chem. Soc., Perkin Trans. 2*, 2000, 1559.
12 W. Kaim, *Angew. Chem., Int. Ed. Engl.*, 1983, **22**, 171; R. Czerwieniec, J. Herbich, A. Kapturkiewicz and J. Nowacki, *Chem. Phys. Lett.*, 2000, **325**, 589.
13 M. C. Zerner, G. H. Loew, R. F. Kirchner and U. T. Mueller-Westerhoff, *J. Am. Chem. Soc.*, 1980, **102**, 589; J. D. Head and M. C. Zerner, *Chem. Phys. Lett.*, 1986, **131**, 359.
14 E. G. McRae, *J. Phys. Chem.*, 1957, **61**, 562; N. S. Bayliss and E. G. McRae, *J. Phys. Chem.*, 1954, **58**, 1002; Y. Oshika, *J. Phys. Soc. Jpn.*, 1954, **9**, 594.
15 D. D. Perrin and W. L. F. Armarego, *Purification of Laboratory Chemicals*, Pergamon Press, Oxford, 3rd edn., 1988.
16 D. J. Darensbourg and R. L. Kump, *Inorg. Chem.*, 1978, **17**, 2680; J. Granifo, *Polyhedron*, 1993, **12**, 27.
17 G. M. Sheldrick, SHELXS-97, Program for Structure Solution, University of Göttingen, Germany, 1997; G. M. Sheldrick, SHELXL-97, Program for the Refinement of Crystal Structures, University of Göttingen, Germany, 1997.
18 L. E. Orgel, *Inorg. Chem.*, 1962, **1**, 25.
19 (*a*) H. J.B. Slot, N. W. Murrall and A. Welch, *Acta Crystallogr., Sect. C*, 1985, **41**, 1309; (*b*) P. N. W. Baxter, J. A. Connor, J. D. Wallis and D. C. Povey, *J. Organomet. Chem.*, 1992, **426**, 187; (*c*) M. A. Bakar, *Acta Crystallogr., Sect. C*, 1993, **49**, 582; (*d*) E. C. Alyea, G. Ferguson and V. K. Jain, *Acta Crystallogr., Sect. C*, 1994, **50**, 854; (*e*) R. S. Herrick, K. L. Houde, J. S. McDowell, L. P. Kiczek and G. Bovaria, *J. Organom. Chem.*, 1999, **589**, 29; (*f*) H. T. Dieck, T. Mack, K. Petrs and H. G. von Schnering, *Z. Naturforsch., B*, 1983, **38**, 568.
20 A. Vlček, Jr., *Coord. Chem. Rev.*, 2002, **230**, 225.
21 R. W. Balk, Th. L. Snoeck, D. J. Stufkens and A. Oskam, *Inorg. Chem.*, 1980, **19**, 3015; P. C. Servaas, H. K. van Dijk, Th. L. Snoeck, D. J. Stufkens and A. Oskam, *Inorg. Chem.*, 1985, **24**, 4494.
22 I. R. Farrell, J. van Slageren, S. Záliš and A. Vlček, Jr., *Inorg. Chim. Acta*, 2001, **315**, 44.
23 S. Záliš, C. Daniel and A. Vlček, Jr., *J. Chem. Soc., Dalton Trans.*, 1999, 3081.
24 H. Saito, J. Fujita and K. Saito, *Bull. Chem. Soc. Jpn.*, 1968, **41**, 863.
25 C. J. F. Böttcher, *Theory of Electric Polarization*, Elsevier, Amsterdam, 1973, vol. 1.
26 (*a*) E. S. Dodsworth and A. B. P. Lever, *Inorg. Chem.*, 1990, **29**, 499; (*b*) E. S. Dodsworth and A. B. P. Lever, *Coord. Chem. Rev.*, 1990, **97**, 271.
27 J. Tomasi and M. Persico, *Chem. Rev.*, 1994, **94**, 2027.
28 L. Onsager, *J. Am. Chem. Soc.*, 1936, **58**, 1486.
29 B. S. Brunschwig, C. Creutz and N. Sutin, *Coord. Chem. Rev.*, 1998, **177**, 61.